Viscoelastic narrowing of a collective mode in molten CsCl observed by inelastic x-ray scattering

2007 J. Phys.: Condens. Matter 19 466110

(http://iopscience.iop.org/0953-8984/19/46/466110)

IOP PUBLISHING JOURNAL OF PHYSICS: CONDENSED MATTER

J. Phys.: Condens. Matter **19** (2007) 466110 (10pp) doi:10.1088/0953-8984/19/46/466110

Viscoelastic narrowing of a collective mode in molten CsCl observed by inelastic x-ray scattering

M Inui[1], S Hosokawa[2], Y Kajihara[1], K Matsuda[3], S Tsutsui[4] and A Q R Baron[4,5]

[1] Graduate School of Integrated Arts and Sciences, Hiroshima University, Higashi-Hiroshima 739-8521, Japan
[2] Center for Materials Research using Third-Generation Synchrotron Radiation Facilities, Hiroshima Institute of Technology, Hiroshima 731-5193, Japan
[3] Graduate School of Engineering, Kyoto University, Kyoto 606-8501, Japan
[4] SPring-8/JASRI 1-1-1 Kouto, Sayo-cho, Sayo-gun, Hyogo 679-5198, Japan
[5] SPring-8/RIKEN 1-1-1 Kouto, Sayo-cho, Sayo-gun, Hyogo 679-5148, Japan

E-mail: inui@mls.ias.hiroshima-u.ac.jp

Received 27 July 2007, in final form 10 September 2007
Published 26 October 2007
Online at stacks.iop.org/JPhysCM/19/466110

Abstract

The dynamic structure factor of molten CsCl has been measured at low momentum transfer, 1.4 $nm^{-1} \leqslant Q < 33$ nm^{-1}, using high-resolution inelastic x-ray scattering. The longitudinal acoustic mode disperses 1.7 times faster than the adiabatic sound velocity and its linewidth increases following the Q^2 law as predicted by the hydrodynamics. However, the linewidth is a factor of seven smaller than the estimation using the linewidths obtained from Brillouin light scattering. The large speed-up and the significant narrowing of the collective mode, which can be related to each other by a recently presented viscoelastic theory, must arise from the intrinsic nature of molten alkali chlorides. Furthermore in comparison with the previous results for molten NaCl and KCl, the apparent sound velocity is found to be approximately scaled by the inverse of the square-root of the effective mass among these molten salts.

(Some figures in this article are in colour only in the electronic version)

1. Introduction

The first observation of a phonon-like peak in liquid rubidium was made more than 30 years ago using inelastic neutron scattering (INS) [1]. One picture to explain the peak is that atoms in a liquid, experiencing backflow by collisions with the surrounding atoms, may move around the equilibrium positions for a short time as if in a crystal. In the case of liquid rubidium, the peak disperses approximately as fast as the adiabatic sound velocity, c_s, consistent with a longitudinal acoustic mode on the atomic scale. However, the presence or absence of such a peak in a liquid is not always simply explained, and its behavior is often not easily related

to macroscopic properties [2–4]. Furthermore, in many cases the peak observed in a liquid disperses faster than c_s. A simple explanation that the solid-like response of a liquid to the high-frequency sound mode on the atomic scale is relevant to the faster dispersion has been proposed based on the viscoelastic theory [5, 6].

Faster dispersion of the acoustic mode may be expected in a liquid with more rigid structure at a short time on the basis of the viscoelastic theory. Here we carry out high-resolution inelastic x-ray scattering (IXS) experiments to observe the dynamics of molten alkali halides, simple binary liquids with solid-like short-range order. The partial structures in molten alkali chlorides have been studied extensively by neutron scattering (NS) using the isotope substitution method with Cl isotopes. The results suggest that molten alkali halides preserve chemical short-range order between cations and anions (charge-ordering) like ionic solids [7].

In this paper we report the results of IXS measurements for molten CsCl. The static and dynamic partial structure factors of molten CsCl were measured by NS [8] and INS [9], respectively. However, INS measurements about 20 years ago could not access the low-Q region in which the longitudinal acoustic mode disperses. Recently high-resolution IXS has been used to investigate atomic dynamics in several molten salts [10–12]. The technique is a powerful tool for studying collective modes at low Q and we could obtain the normalized dynamic structure factor, $S(Q, \omega)/S(Q)$, in 1.4 nm$^{-1} \leqslant Q < 33$ nm^{-1}, where Q and ω represent momentum and energy transfer, respectively. We find that a distinct acoustic mode disperses much faster than c_s and the linewidth of the mode is reduced by a factor of seven compared to expectations from Q^2 scaling of the Brillouin linewidth reported by Qiu *et al* [13]. We conclude that both the faster dispersion and narrowing of the acoustic mode in molten CsCl must be explained by the intrinsic nature of the molten salt from the estimation on the basis of a viscoelastic theory recently presented by Scopigno *et al* [2, 14].

2. Experimental details

This experiment was conducted at the high-resolution IXS beamline (BL35XU) of SPring-8 in Japan [15]. Backscattering at the Si(11 11 11) reflection was used to provide a beam of 4×10^9 photons s^{-1} in a 0.8 meV bandwidth onto the sample. The energy of the incident beam and the Bragg angle of the backscattering were 21.747 keV and approximately 89.98°, respectively. We used 12 spherical analyzer crystals at the end of the 10 m horizontal arm. The spectrometer resolution was 1.5–1.8 meV depending on the analyzer crystal as measured using scattering from polymethyl methacrylate (PMMA). The momentum transfer resolution, ΔQ, was 0.45 nm^{-1} at $Q < 11$ nm^{-1}, and 1.0 nm^{-1} at $Q > 11$ nm^{-1}.

The CsCl sample of 99.999% purity and 0.2 mm thickness (approximately equal to the optical depth at 2.7 g cm^{-3}) was mounted in a single-crystal sapphire cell modified from the original one [16]. The cell was contained in a chamber with wide windows made of thin single-crystalline Si which was replaced with a Be plate of the original design [17] to reduce the background from the window. The chamber was filled with 2 bar of He gas (99.9999% purity) to reduce evaporation of molten CsCl. IXS spectra of molten CsCl were measured at 993 K (the melting temperature is 919 K). Scans over a range from −50 to 50 meV required 3 h, with total data collection times of 24, 18 and 24 h for $Q < 5.5$ nm^{-1}, 6.7 nm$^{-1} < Q < 11$ nm^{-1} and 11 nm$^{-1} < Q < 33$ nm^{-1}, respectively. Backgrounds were measured at the same temperature and Q positions using the empty cell.

3. Results

We obtained the IXS spectra of molten CsCl, $I(Q, \omega)$, after subtracting the background from the observed data with absorption correction and deduced $S(Q, \omega)/S(Q)$ from normalizing

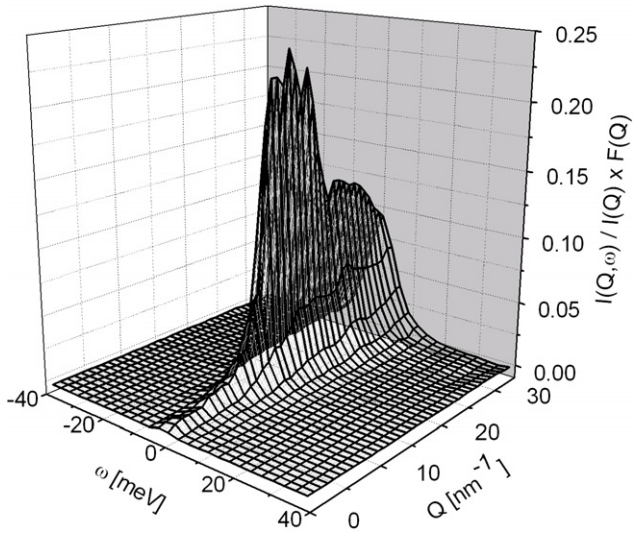

Figure 1. A perspective plot of $I(Q,\omega)/I(Q)\times F(Q)$ of molten CsCl.

$I(Q,\omega)$ by $I(Q)$, the energy integral of $I(Q,\omega)$. Figure 1 shows a perspective plot of $S(Q,\omega)/S(Q)\times F(Q)$, where $F(Q)$ is the total scattering intensity including the incoherent component which is calculated from the partial structure factors [8] and the atomic form factors of Cs and Cl. Figure 2(a) shows $S(Q,\omega)/S(Q)$ in the low-Q region. A distinct shoulder is observable on both sides of the elastic part, $S(Q,0)/S(Q)$, and it shifts to higher ω with increasing Q to 6 nm^{-1}. Figure 2(b) shows $S(Q,\omega)/S(Q)$ in the high-Q region. The quasielastic peak becomes narrow at approximately 15 nm^{-1} around the $F(Q)$ maximum similar to de Gennes narrowing in monatomic liquids. For $Q > 15$ nm^{-1}, the profile of $S(Q,\omega)/S(Q)$ becomes broad and the inelastic components are merged into the quasielastic peak. As shown in figure 3(a), $I(Q)$ agrees well with $F(Q)$.

The observed $S(Q,\omega)/S(Q)$ is broadened by the spectrometer resolution. To deconvolute the observed spectra, we used a model function composed of a pseudo-Voigt function for the quasielastic peak, $F_{\rm qel}(Q,\omega)$, and damped harmonic oscillator (DHO) for inelastic excitations, $F_{\rm inel}(Q,\omega)$. The model function is expressed by,

$$\begin{aligned} S(Q,\omega)/S(Q) &= B(\omega')[F_{\rm qel}(Q,\omega') + F_{\rm inel}(Q,\omega')]\otimes R(\omega-\omega'),\\ F_{\rm qel}(Q,\omega) &= \frac{(1-c)A_0}{\pi}\frac{\Gamma_{\rm L}}{\Gamma_{\rm L}^2+\omega^2} + \frac{cA_0}{\Gamma_{\rm G}}\sqrt{\frac{\ln 2}{\pi}}\exp\left[-\ln 2\left(\frac{\omega}{\Gamma_{\rm G}}\right)^2\right],\\ F_{\rm inel}(Q,\omega) &= \frac{A_1}{\pi\beta\hbar}\frac{4\omega_Q\Gamma_Q}{(\omega^2-\Omega_Q^2)^2+4\omega^2\Gamma_Q^2}, \end{aligned} \tag{1}$$

where $B(\omega) = \beta\hbar\omega/\left[1-\exp(-\beta\hbar\omega)\right]$, $\beta = (k_{\rm B}T)^{-1}$ and $\omega_Q = \sqrt{\Omega_Q^2-{\Gamma_Q}^2}$. A_0, c, $\Gamma_{\rm L}$ and $\Gamma_{\rm G}$ are the amplitude, Gaussian fraction and the widths of Lorentzian and Gaussian components, respectively. A_1, Γ_Q and Ω_Q are the amplitude, the width and the excitation energy for the inelastic peak. The symbol $\otimes$ indicates convolution with the resolution function, $R(\omega)$. We carried out the least-square fitting using the model function. The optimized convolution and deconvolution are indicated in figure 2(a) by bold and thin solid lines, respectively. The large fraction of $F_{\rm qel}(Q,\omega)$ in the fits may originate from the fact that the

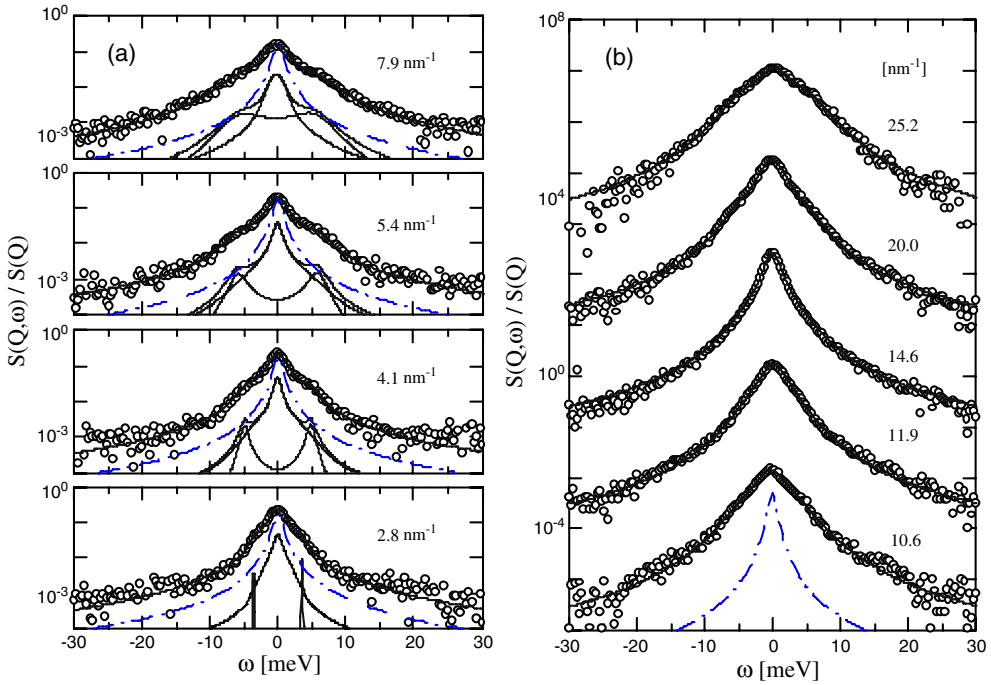

Figure 2. (a) $S(Q, \omega)/S(Q)$ of molten CsCl at 993 K (open circles) and fits (bold solid lines on the data points) made by the model function in the low-Q region. Also shown are a model function (bold solid lines), the quasielastic (thin solid curves) and inelastic (thin solid curves) peaks, and the resolution function (dash–dotted curves). (b) $S(Q, \omega)/S(Q)$ (open circles) and fits (bold solid lines) in the high-Q region. Each spectrum is multiplied by 10^2 for clarity. Also shown is the resolution function (dash–dotted curves).

observed $S(Q, \omega)/S(Q)$ has, effectively, an incoherent component because of large difference in the atomic form factors between Cs and Cl.

$S(Q, \omega)/S(Q)$ in molten CsCl is well reproduced by the present simple model of the quasielastic peak and a single DHO component while the total $S(Q, \omega)/S(Q)$ is composed of Cs–Cs, Cs–Cl and Cl–Cl correlations and is strongly weighted by the components including Cs with a large scattering amplitude. The average value of χ-square per degree of freedom with the standard deviation is 1.3 ± 0.3, suggesting reasonably good fits. Why can the present model reproduce the present data? The reason may be explained as follows. As the previous structural studies on molten alkali halides have suggested [7–9], the cation–cation and anion–anion partial structure factors, S_{++} and S_{--}, respectively, are approximately equivalent in molten alkali halides. In this case, one can take the density–density correlation function, $S_{nn} = S_{++} + S_{+-}$, and charge–charge correlation function, $S_{qq} = S_{++} - S_{+-}$, where S_{+-} is the cation–anion partial structure factor, as two independent partial structure factors instead of S_{++}, S_{--} and S_{+-} [9]. The collective excitations in S_{nn} and S_{qq} correspond to a longitudinal acoustic mode and an optic-like mode, respectively, in molten alkali halides. We speculate that the former excitation must be obtained from the present analysis since the latter excitation is known to be very difficult to observe [11]. In the next section we discuss the present results regarding the excitations represented by the DHO component at Q lower than the $F(Q)$ maximum as the longitudinal sound mode in S_{nn}.

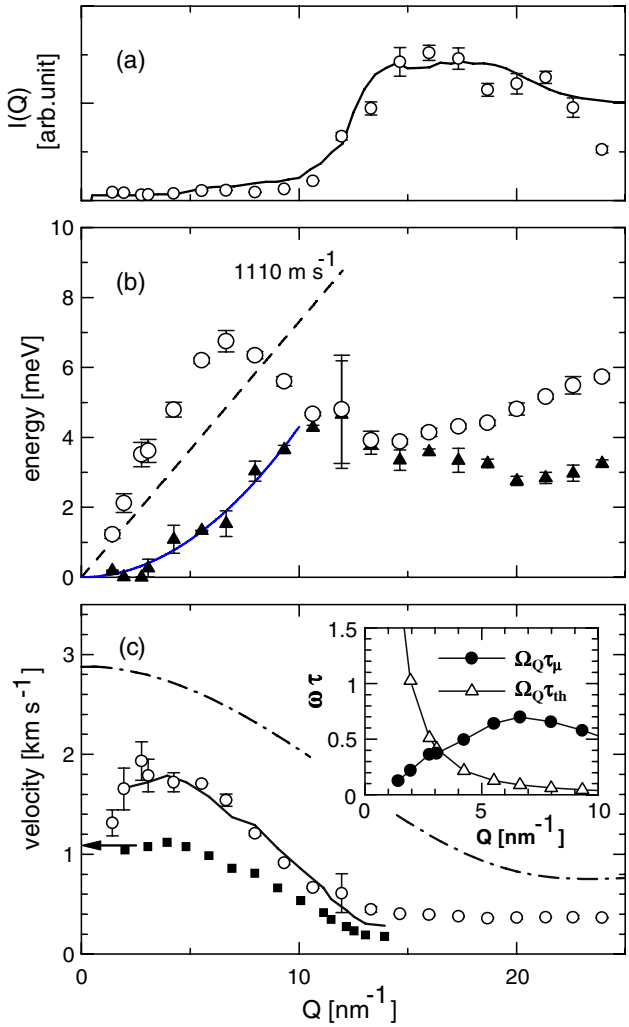

Figure 3. (a) The integrated intensity of $I(Q, E)$, $I(Q)$ (open circles), normalized by the polarization factor, and total scattering intensity $F(Q)$ (solid curve). (b) Ω_Q (open circles) and Γ_Q (closed triangles) obtained from the least-squares fits using the model function. Also shown are a fitting curve of Γ_Q with $W_{\mathrm{IXS}}\,Q^2$ (solid curve) and a dispersion with a slope of 1110 m s^{-1} (broken line). (c) $c_Q(Q)$ (open circles), $c_\infty(Q)$ (dash–dotted curve) and c_s (arrow) of molten CsCl. Also shown are $c_Q(Q)$ (solid squares) of liquid Cs taken from [27], and that multiplied by 1.6 (solid line). The inset shows the excitation frequency multiplied by the structural and thermal relaxation time, $\Omega_Q\tau_\mu$ and $\Omega_Q\tau_{\mathrm{th}}(Q)$, respectively.

4. Discussion

We plot Ω_Q and Γ_Q as a function of Q in figure 3(b). Ω_Q shows nearly linear dispersion at low Q and has a minimum around 15 nm^{-1} at around the $F(Q)$ maximum. With further increasing Q, Ω_Q starts to increase again. Ω_Q in the low-Q region disperses faster than c_s (1110 m s^{-1} [18]), denoted by a broken line in the figure. The apparent sound velocity, $c_Q(Q) = \Omega_Q/Q$, is plotted in figure 3(c) with c_s indicated by the arrow. Also shown is the high-frequency sound speed (a dash–dotted line), $c_\infty(Q) = \omega_{\mathrm{LA}}(Q)/Q$, which is calculated

Table 1. Q^2 scaling factors for the linewidth of the acoustic mode in molten CsCl obtained by several methods.

Q^2 scaling factor ($m^2\ s^{-1}$)	Methods
$2W = 1.3\times10^{-5}$	Equation (2) with η_B
$2W' = 7.7\times10^{-7}$	Equation (2) without η_B
$2W^{obs} = 9.8\times10^{-7}$	BLS [13]
$2W_{IXS} = 1.3\times10^{-7}$	The present IXS

using a formula deduced from the exact normalized fourth frequency moment, $\omega_{LA}(Q)$, in molten alkali halides, given in [19]. To calculate $\omega_{LA}(Q)$ we use the approximation similar to the monatomic liquids [20] neglecting the term for the plasma oscillation, and including the interionic distance of 0.34 nm and the Einstein frequency of 10 meV evaluated from the literature [21, 22]. $c_Q(Q)$ increases with increasing Q up to 3 nm^{-1} and starts to decrease at 6 nm^{-1}. The maximum of $c_Q(Q)$ is about 1900 m s^{-1}, which is 71% faster than c_s. This speed-up is much larger than the 10–20% reported in many liquid metals. Such a large speed-up of $c_Q(Q)$ was also reported in other molten alkali halides by IXS studies [10, 12]. As for the linewidth of the acoustic mode, Γ_Q increases following the Q^2 law as the generalized hydrodynamics predicts. When we define $\Gamma_Q = W_{IXS}Q^2$, the optimized W_{IXS} of 0.043 ± 0.004 meV nm^2 is obtained.

On the macroscopic scale, the acoustic mode can be observed by Brillouin light scattering (BLS). Hydrodynamics expresses the Brillouin linewidth Γ_{BLS} using the equation [5, 6]

$$\begin{aligned} &\Gamma_{BLS} = WQ^2, \\ &W = \tfrac{1}{2}\{(\tfrac{4}{3}\eta + \eta_B)/\rho + (\gamma - 1)D_T\}, \end{aligned} \tag{2}$$

where η, η_B, ρ, γ and D_T are shear and bulk viscosities, mass density, the specific heat ratio and the thermal diffusivity, respectively. Here D_T is represented by $D_T = \lambda/(\rho C_p)$, where C_p and λ are the specific heat at constant pressure and thermal conductivity, respectively. Equation (2) means that the dissipation to viscous and thermal decay channels determines the linewidth.

Qiu *et al* [13] investigated the acoustic mode in molten CsCl at very low Q using a BLS technique. They found the position of the Brillouin peak consistent with the prediction from c_s of molten CsCl. However, the Brillouin linewidth was not consistent with the one given by equation (2). The results are summarized in table 1. When $\eta = 1.3$ mPa s, $\eta_B = 32$ mPa s, $\gamma = 1.5$, $C_p = 450$ J K^{-1} kg^{-1} [18] and $\lambda = 0.31$ W m^{-1} K^{-1} [23] are used, W becomes approximately an order larger than W^{obs} observed by BLS. Qiu *et al* pointed out that this discrepancy may be due to large η_B with less reliability. In fact W' obtained by neglecting η_B is in fairly good agreement with W^{obs}. This fact means that W^{obs} may be consistent with equation (2) if the real η_B is smaller than the reported one, as Qiu *et al* speculated. However, W_{IXS} obtained in the present study is approximately a factor seven smaller than W^{obs}, as shown in table 1.

This narrow W_{IXS} does not seem to be a result of correlations between the optimized parameters. We used $F_{qel}(Q, \omega)$ of the pseudo-Voigt function because $F_{qel}(Q, \omega)$ of a simple Lorentzian did not reproduce the observed spectra at higher Q around de Gennes narrowing, while it worked at low Q where Ω_Q disperses linearly and the optimized c is less than 0.2. When the simple Lorentzian was used for $F_{qel}(Q, \omega)$, we obtained 0.045 meV nm^2 as a Q^2 scaling factor for Γ_Q, which is consistent with the present result within the error bar.

The IXS results of molten CsCl are summarized as the speed-up of $c_Q(Q)$ at low Q and the linewidth of the acoustic mode smaller than the hydrodynamic equation. Similar results have already been reported in several liquid metals. Scopigno *et al* [2] discussed the applicability of

equation (2) for IXS data of liquid Li and related the speed-up and the small linewidth to the structural relaxation based on the viscoelastic theory. They assumed the memory function constituted of slow (α) and fast (μ) structural relaxations, and a thermal one (th), whose relaxation times are τ_α, τ_μ and $\tau_{\rm th}$, respectively. They took the simple Debye approximation and gave the memory function, $M(Q,t)$, by

$$M(Q,t) = \Delta_\alpha^2 \mathrm{e}^{-t/\tau_\alpha} + \Delta_\mu^2 \mathrm{e}^{-t/\tau_\mu} + \Delta_{\rm th}^2 \mathrm{e}^{-a(Q)Q^2 t}, \tag{3}$$

where $a(Q)$ corresponds to $D_{\rm T}$ in the $Q\to 0$ limit and $\tau_{\rm th}(Q) = (a(Q)Q^2)^{-1}$. In their theory, $c_Q(Q)$ faster than $c_{\rm s}$ is related to the pole of the Fourier–Laplace transform of $M(Q,t)$ and does not exceed the high-frequency sound speed, $c_\infty(Q)$, represented by $\pm\mathrm{i}\sqrt{\omega_0^2 + \Delta_{\rm th}^2 + \Delta_\alpha^2 + \Delta_\mu^2} = \pm\mathrm{i}c_\infty(Q)Q$, while $c_{\rm s}$ is expressed by $\pm\mathrm{i}\sqrt{\omega_0^2 + \Delta_{\rm th}^2} = \pm\mathrm{i}c_{\rm s}Q$, where ω_0^2 is the normalized second frequency moment of $S(Q,\omega)$. They assumed that the α-process, slow enough to be frozen, is not responsible for Q dependence of $c_Q(Q)$ and the observed speed-up is caused by the μ-process. In respect to the linewidth of the sound mode, they replaced $(4\eta/3 + \eta_{\rm B})/\rho$ representing the viscous decay with $\Delta_\mu^2\tau_\mu/Q^2$ in equation (2) for the same reason that the slow α process could not contribute to the damping of the sound modes.

We analyze the present results based on their theory. We assume $2W_{\rm IXS} = \Delta_\mu^2\tau_\mu/Q^2$ by neglecting the term of $(\gamma - 1)D_{\rm T}$ in equation (2) because λ is much smaller in molten CsCl than in liquid metals. We will discuss this assumption below. Next we estimate Δ_μ^2 from the observed increase of $c_Q(Q)$ at low Q using the approximation of $\Delta_\mu^2/Q^2 \simeq c_Q^2(2.8) - c_Q^2(1.4)$. Then we can obtain $\tau_\mu = 0.07$ ps, which is of the same order as τ_μ in liquid Li [2]. The inset of figure 3(c) shows $\Omega_Q\tau_\mu$ and $\Omega_Q\tau_{\rm th}(Q)$ as a function of Q up to 10 nm^{-1}. We calculate $\tau_{\rm th}(Q)$, assuming $a(Q) = D_{\rm T}$. As seen in the inset, $\Omega_Q\tau_\mu$ is smaller than unity but clearly correlated with $c_Q(Q)$. Large $\Omega_Q\tau_{\rm th}(Q)$ at low Q suggests the adiabatic propagation of the sound mode. We assume that $\Delta_{\rm th}^2$ does not change from 1.4 to 2.8 nm^{-1} because the transition from the adiabatic to the isothermal propagation will shift to higher Q than the Q corresponding to $\Omega_Q\tau_{\rm th}(Q) = 1$, as recently reported in [24]. If a thermal decay denoted by $(\gamma - 1)D_{\rm T}$ is included in the estimation, $\Delta_\mu^2\tau_\mu/Q^2$ becomes very small, and τ_μ of the order of 1 fs is obtained. Such extremely fast relaxation cannot explain the observed variation of $c_Q(Q)$ at low Q. The present estimation may indicate that the thermal decay channel does not make a major contribution to the linewidth, probably because the generalized specific heat ratio, $\gamma(Q)$, already approaches unity at the lowest Q in the present data. Of course, neglecting the thermal decay channel must not present the real relaxation exactly, but even if we take account of it properly, it should be concluded that the fast structural relaxation with τ_μ less than 0.1 ps is strongly relevant to the present results.

Large speed-up of $c_Q(Q)$ was also reported by the previous IXS studies on molten alkali halides. Demmel *et al* [10] found for the first time that the fast dispersion of the apparent sound velocity in molten NaCl is similar to the dispersion in liquid Na, and discussed that the fast dispersion might be related to a fast sound mode derived from lighter alkali atoms. Their investigations on molten KCl [12] confirmed the similarity of the dispersion between molten alkali halides and liquid alkali metals again. Because the influence of S_{qq} on the total scattering intensity is negligible in molten KCl, the fast dispersion must arise from S_{nn}. To understand the similarity of the apparent sound velocity, Demmel *et al* [12] speculated about a plasmon-type mode of the cations on a uniform anion background mediated by the polarized electron clouds of the anions. In practice, a plasmon-type theory originally presented by Bohm and Staver [25] is known to explain a longitudinal collective mode in alkali metals, and recently the applicability of the theory to collective dynamics in a liquid K–Cs alloy was reported [26].

Table 2. A scaling factor of the apparent sound velocity deduced from the particle mass, $\sqrt{M_+/2m_r}$, where M_+ and $2m_r$ are the cation and the effective mass, respectively. The reduced mass m_r is given by $m_r = M_+M_-/(M_+ + M_-)$. Here the Cl mass M_- is 35.5. Also indicated are the experimental data of c_{salt}/c_{metal} for $c_Q(Q)$ and c_s, and $c_Q(Q)\sqrt{2m_r}$. The results of molten NaCl and KCl are quoted from [10] and [12], respectively. c_s of liquid alkali metals is taken from [28].

	NaCl	KCl	CsCl
M_+	23.0	39.1	132.9
$2m_r$	27.9	37.2	56.0
$\sqrt{M_+/2m_r}$	0.91	1.03	1.54
c_{salt}/c_{metal} for $c_Q(Q)$	∼1	∼1	1.6
c_{salt}/c_{metal} for c_s	0.70	0.89	1.15
$c_Q(Q)\sqrt{2m_r}$ (km s^{-1})	15.3	14.4	14.2

Although the similarity of the dispersion to pure liquid alkali metals was observed in molten NaCl and KCl, this is not the case in molten CsCl. $c_Q(Q)$ of molten CsCl is much faster than that of liquid Cs [27], as seen in figure 3(c). Meanwhile, when the velocity is in inverse proportion to the square-root of particle mass, the ratio of the sound velocity may follow the equation given by

$$c_{salt}/c_{metal} = \sqrt{M_+/2m_r}, \tag{4}$$

where c_{salt}, c_{metal}, M_+ and $2m_r$ denote the sound velocities of a molten salt and a liquid metal, the cation mass and the effective mass (m_r is the reduced mass) [19, 26], respectively. As seen in figure 3(c), $c_Q(Q)$ of molten CsCl is scaled by a factor 1.6 to that of liquid Cs. This scaling factor is approximately equal to a factor 1.54 deduced from equation (4) as indicated in table 2. Interestingly the scaling factors of NaCl and KCl in table 2 calculated from equation (4) are approximately unity, which indicates that the previous experimental results may also follow equation (4). A physical picture of equation (4) means that quasi-particles with the effective mass move collectively in the molten salt as if they were atoms in the liquid metal. A cooperative motion of the cations and anions is inferred from this picture. We may not need to assume a plasmon-type mode of the cations on a uniform anion background to explain the fast dispersion in molten NaCl and KCl. Furthermore $c_Q(Q)$ normalized by the inverse of the square-root of the effective mass, $c_Q(Q)\sqrt{2m_r}$, is approximately constant among these three molten salts as indicated in table 2. The picture of a quasi-particle dynamics may commonly be applied to these molten salts. Here we have a question: why does $c_Q(Q)$ seem to follow equation (4) despite the electronic properties being very different between liquid metals and molten salts? Note that the adiabatic sound velocity in these systems does not seem to follow equation (4) as indicated in table 2. We consider the question from a microscopic point of view and point out that the average interatomic distance in the liquid alkali metals [29] is approximately as large as the average interionic distance of like ions in these molten alkali halides [7]. The average interionic distance of like ions is equivalent to the average distance of the quasi-particles in the molten salt. This experimental fact may be related to the result that equation (4) is useful to estimate $c_Q(Q)$ of the molten salt from that of the corresponding liquid metal while the results following equation (4) may be fortuitous.

On the basis of the above discussion we try to explain the present experimental results by a theory applicable to these molten salts, which may be the viscoelastic theory. The present results for molten CsCl indicate that $c_Q(Q)$ is much faster than the adiabatic sound velocity and a similar behavior is observed in molten NaCl and KCl, suggesting that it is a common phenomenon independent of the cation species. We may be able to relate the large speed-up of $c_Q(Q)$ and narrowing of W_{IXS} to the charge-ordering intrinsic to molten alkali halides.

We speculate that the charge-ordering enhances the elastic property of the molten salts on the atomic scale and promotes a cage-effect. The cage-effect is a crucial idea for understanding liquid dynamics near the triple point. It has been used to explain negative values of the velocity autocorrelation function obtained from molecular dynamics simulations and to classify the liquid dynamics into the fast (μ) process related to backflow due to binary collisions with the surrounding particles and the slow (α) one related to escape motions from the cage [5, 6]. The large speed-up of $c_Q(Q)$ and small linewidths of the acoustic mode in molten CsCl must originate from the rigid cage formed by the charge-ordering.

The charge-ordering in molten salts has been related to the theoretical prediction that an optic-like mode similar to ionic solids may exist as well as the well defined longitudinal acoustic mode [30] (also see references in [7, 11]). However the INS results [9] suggest that the optic-like modes in molten CsCl are strongly damped for $Q > 15$ nm^{-1}. While a large difference in the atomic form factors between Cs and Cl may be advantageous for observing the optic-like mode [11], we also could not find distinct excitations of the optic-like mode in the observed IXS spectra and were not successful in finding evidence for optic-like modes in molten CsCl. The results of fitting the present $S(Q, \omega)/S(Q)$ using a model function with double DHO components show that the second inelastic peak could be included at $\sim$13$\pm$2 meV and around 13 nm^{-1} near the maximum of the charge–charge correlation function [9]. However, its amplitude was negligibly small and its energy did not disperse to either side of the Q. This may simply imply that it is difficult to observe the optic-like modes. Otherwise the present results may indicate that the point-charge approximation used in many theoretical studies is not correct for molten CsCl.

5. Summary

IXS measurements of molten CsCl show a large speed-up of the apparent sound velocity and small linewidths of the acoustic mode. Using a viscoelastic theory recently presented by Scopigno *et al* [2, 14], we estimate a relaxation time of less than 0.1 ps corresponding to the fast (μ) structural relaxation due to binary collisions with the surrounding particles in molten CsCl. The charge-ordering in the molten salt must play a crucial role for the large speed-up and the strong reduction of the damping in the acoustic mode. Meanwhile we have found that the apparent sound velocity of molten CsCl and liquid Cs is approximately scaled by the inverse ratio of the square-root of particle mass and a similar relation is obtained from the data of molten NaCl and KCl. In addition, $c_Q(Q)$ normalized by $1/\sqrt{2m_r}$ is found to be approximately constant among these molten salts. It is a subject for future work to understand why the apparent sound velocity in the different systems follows such a scaling law and how the scaling law is relevant to the viscoelastic theory explaining the present results. Further analysis using the memory function formalism for binary liquids [31] may be useful for a deeper understanding of coherent dynamics in molten alkali halides.

Acknowledgments

The authors would like to thank Professor S Takeda for valuable discussion and Mr Y Azumi for experimental support. This work is supported by a Grant-in-Aid for Scientific Research from the Ministry of Education, Science and Culture, Japan. The synchrotron radiation experiment was performed at the SPring-8 with the approval of the Japan Synchrotron Radiation Research Institute (JASRI) (proposal no. 2006B1146).

References

[1] Copley J R D and Rowe J M 1974 *Phys. Rev. Lett.* **32** 49
[2] Scopigno T, Balucani U, Ruocco G and Sette F 2000 *J. Phys.: Condens. Matter* **12** 8009
[3] Scopigno T, Filipponi A, Krisch M, Monaco G, Ruocco G and Sette F 2002 *Phys. Rev. Lett.* **89** 255506
[4] Scopigno T, Ruocco G and Sette F 2005 *Rev. Mod. Phys.* **77** 881
[5] Boon J P and Yip S 1980 *Molecular Hydrodynamics* (New York: McGraw-Hill)
[6] Balcani U and Zoppi M 1994 *Dynamics of the Liquid State* (Oxford: Clarendon)
[7] McGreevy R L 1987 *Solid State Phys.* **40** 247
[8] Locke J, Messoloras S, Stewart R J, McGreevy R L and Mitchell E W J 1985 *Phil. Mag.* B **51** 301
[9] McGreevy R L, Mitchell E W J, Margaca F M and Howe M A 1985 *J. Phys. C: Solid State Phys.* **18** 5235
[10] Demmel F, Hosokawa S, Lorenzen M and Pilgrim W-C 2004 *Phys. Rev.* B **69** 012203
[11] Demmel F, Hosokawa S, Pilgrim W-C and Tsutsui S 2005 *Nucl. Instrum. Methods Phys. Res.* B **238** 98
[12] Demmel F, Hosokawa S and Pilgrim W-C 2007 *J. Alloys Compounds* at press (Available online 20 January 2007)
[13] Qiu S L, Bunten R A J, Dutta M, Mitchell E W J and Cummins H Z 1985 *Phys. Rev.* B **31** 2456
[14] Scopigno T and Ruocco G 2004 *Phys. Rev.* E **70** 013201
[15] Baron A Q R, Tanaka Y, Goto S, Takeshita K, Matsushita T and Ishikawa T 2000 *J. Phys. Chem. Solids* **61** 461
[16] Tamura K, Inui M and Hosokawa S 1999 *Rev. Sci. Instrum.* **70** 144
[17] Hosokawa S and Pilgrim W C 2001 *Rev. Sci. Instrum.* **72** 1721
[18] Janz G J 1967 *Molten Salts Handbook* (New York: Academic)
[19] Adams E M, McDonald I R and Singer K 1977 *Proc. R. Soc.* A **357** 37
[20] Copley J R D and Lovesey S W 1975 *Rep. Prog. Phys.* **38** 461
[21] Papatheodorou G N, Kalogrianitis S G, Mihopoulos T G and Pavlatou E A 1996 *J. Chem. Phys.* **105** 2660
[22] Ribeiro M C C and Madden P A 1997 *J. Chem. Phys.* **106** 8616
[23] Cornwell K 1971 *J. Phys. D: Appl. Phys.* **4** 441
[24] Bencivenga F, Cunsolo A, Krisch M, Monaco G, Ruocco G and Sette F 2006 *Europhys. Lett.* **75** 70
[25] Bohm D and Staver T 1951 *Phys. Rev.* **84** 836
[26] Bove L E, Sacchetti F, Petrillo C and Dorner B 2000 *Phys. Rev. Lett.* **85** 5352
[27] Bodensteiner T, Morkel Chr, Gläser W and Dorner B 1992 *Phys. Rev.* A **45** 5709
[28] Ohse W 1985 *Handbook of Thermodynamic and Transport Properties of Alkali Metals* (Oxford: Blackwell Scientific)
[29] Waseda Y 1980 *The Structure of Non-crystalline Materials* (New York: McGraw-Hill)
[30] Hansen J P and McDonald I R 1975 *Phys. Rev.* A **11** 2111
[31] Anento N, González L E, González D J, Chushak Y and Baumketner A 2004 *Phys. Rev.* E **70** 041201